

# Interface tool from Wannier90 to RESPACK: **wan2respack**

Kensuke Kurita<sup>a</sup>, Takahiro Misawa<sup>b,c</sup>, Kazuyoshi Yoshimi<sup>b</sup>, Kota Ido<sup>b</sup>, Takashi Koretsune<sup>a</sup>

<sup>a</sup>*Department of Physics, Tohoku University, Sendai 980-8578, Japan*

<sup>b</sup>*The Institute for Solid State Physics, The University of Tokyo, Chiba 277-8581, Japan*

<sup>c</sup>*Beijing Academy of Quantum Information Sciences, Haidian District, Beijing 100193, China*

---

## Abstract

We develop the interface tool **wan2respack**, which connects **RESPACK** (software that derives the low-energy effective Hamiltonians of solids) with **Wannier90** (software that constructs Wannier functions). **wan2respack** converts the Wannier functions obtained by **Wannier90** into those used in **RESPACK**, which is then used to derive the low-energy effective Hamiltonians of solids. In this paper, we explain the basic usage of **wan2respack** and show its application to standard compounds of correlated materials, namely, the correlated metal  $\text{SrVO}_3$  and the high- $T_c$  superconductor  $\text{La}_2\text{CuO}_4$ . Furthermore, we compare the low-energy effective Hamiltonians of these compounds using Wannier functions obtained by **Wannier90** and those obtained by **RESPACK**. We confirm that both types of Wannier functions give the same Hamiltonians. This benchmark comparison demonstrates that **wan2respack** correctly converts Wannier functions in the **Wannier90** format into those in the **RESPACK** format.

**Keywords:** Wannier functions, *ab initio* downfolding, constrained random phase approximation, strongly correlated electron systems

---

## PROGRAM SUMMARY

Program title: **wan2respack**

Licensing provisions: GNU General Public License version 3

Programming language: Fortran and python3

Computer: PC, cluster machine

Operating system: Unix-like system, tested on Linux and macOS

Keywords: Wannier functions, *ab initio* downfolding, constrained random phase approximation, strongly correlated electron systems.

External routines/libraries: Quantum ESPRESSO (version 6.6), **Wannier90** (version 3.0.0), **RESPACK** (version 20200113), **tomli**.

Nature of problem: Using **RESPACK**, one can derive low-energy effective Hamiltonians of solids from maximally localized Wannier functions. However, due to the differences in the representation of Wannier functions, the Wannier functions obtained by **Wannier90** cannot be directly used in **RESPACK**.

Solution method: **wan2respack** converts the Wannier functions in the **Wannier90** format into those in the **RESPACK** format. Using the converted Wannier functions, one can derive the low-energy effective

Hamiltonians using **RESPACK**.

## 1. Introduction

Wannier functions, constructed through unitary transformations of Bloch functions, offer simple, convenient representations of the electronic structures of solids [1]. After the development of an efficient method of obtaining unique sets of maximally localized Wannier functions (MLWFs) [2, 3], MLWFs have been widely used to analyze the electronic structures of solids. For example, MLWFs play an essential role in calculating electronic polarizations [4, 5] and orbital magnetizations [6, 7]. MLWFs are also used to construct tight-binding models [8], which reproduce low-energy bands near the Fermi level.

MLWFs are also vital for deriving the *ab initio* low-energy effective Hamiltonians of solids [9, 10]. Based on MLWFs, the screened interactions in low-energy effective Hamiltonians are evaluated through constrained random phase approximation (cRPA). The derivation of low-energy ef-

fective Hamiltonians is often called *ab initio* downfolding. Correlation effects beyond the conventional density functional theory (DFT) [11, 12] can be considered by solving low-energy effective Hamiltonians using accurate solvers. In the last decade, this method has been applied to a wide range of strongly correlated compounds [13–38].

The open-source software package **Wannier90** [39–42] was developed to construct MLWFs from the results of *ab initio* band calculations. The MLWFs obtained by **Wannier90** can be used to calculate many important properties of solids, such as Berry phases and anomalous Hall conductivity [43], electrical conductivity [44], and spin Hall conductivity [45]. Because of this versatility, many *ab initio* calculation software packages, such as **Quantum ESPRESSO** [46, 47], **VASP** [48, 49], **WIEN2k** [50], **ABINIT** [51], and **OpenMX** [52–54], have an interface to **Wannier90**.

Nakamura *et al.* recently developed the open-source software package **RESPACK** [55, 56], which implements *ab initio* downfolding. After its release, **RESPACK** has been applied to a wide range of correlated materials [57–71]. **RESPACK** also provides functions (**RESPACK-Wannier**) that construct MLWFs using the *ab initio* band calculation results obtained by **Quantum ESPRESSO** or **xTAPP** [72, 73]. The **RESPACK-Wannier** code was developed independently of **Wannier90**. Therefore, their representation of Wannier functions has technical differences, such as the choice of  $k$ -point mesh (e.g., based on irreducible or reducible representation), although the constructed Wannier functions themselves are equivalent. Due to these differences, **RESPACK** cannot be directly connected with **Wannier90**.

In this paper, we introduce the interface tool **wan2respac** [74], which converts Wannier functions in the **Wannier90** format into those in the **RESPACK** format. After the conversion of Wannier functions, the screened Coulomb and exchange interactions can be evaluated using **RESPACK**. The rest of this paper is organized as follows. In Section 2, we give an overview of the formats of the MLWFs implemented in **Wannier90** and **RESPACK** and explain how to convert them using **wan2respac**. We also explain how to derive low-energy effective Hamiltonians based on the converted MLWFs. In Sections 3 and 4, we explain the installation and usage, respectively, of **wan2respac**. In Section 5, we show the application of **wan2respac** to the correlated materials  $\text{SrVO}_3$  and  $\text{La}_2\text{CuO}_4$ . Section 6 summarizes this paper.

## 2. Overview

This section provides an overview of the formats of the Wannier functions implemented in **Wannier90** and **RESPACK**. We also explain how **wan2respac** converts Wannier functions in the **Wannier90** format into those in the **RESPACK** format. Finally, we discuss how to derive the low-energy effective Hamiltonians of solids based on the converted MLWFs.

We obtain MLWFs through unitary transformations of Bloch functions. The Wannierization procedure consists of the following optimization of two quantities:

1. Projection  $[U(\mathbf{k})_{mn}^{\text{opt}}$  in Eq. (1)] of the Bloch functions within the given energy window to minimize the gauge-invariant Wannier spread
2. Unitary transformation  $[U_{im}(\mathbf{k})$  in Eq. (2)] of the optimal Bloch wave functions ( $\psi_{m\mathbf{k}}^{\text{opt}}(\mathbf{k})$  in Eq. (2)) obtained by the first step

According to the Wannierization procedure, the  $i$ th Wannier function around site  $\mathbf{R}$  ( $\mathbf{R}$  is often called the Wannier center),  $w_{i\mathbf{R}}(\mathbf{r}) = w_{i0}(\mathbf{r} - \mathbf{R})$ , is defined as

$$w_{i\mathbf{R}}(\mathbf{r}) = \frac{1}{\sqrt{N_{\mathbf{k}}}} \sum_{\mathbf{k}} \sum_m U_{im}(\mathbf{k}) \psi_{m\mathbf{k}}^{\text{opt}}(\mathbf{r}) e^{-i\mathbf{k} \cdot \mathbf{R}}, \quad (1)$$

where  $N_{\mathbf{k}}$  is the number of  $\mathbf{k}$ -point meshes and  $U_{im}(\mathbf{k})$  is the unitary matrix, which transforms the  $m$ th optimized Bloch wave function  $\psi_{m\mathbf{k}}^{\text{opt}}(\mathbf{r})$  into the  $i$ th Wannier function. Here,  $\psi_{m\mathbf{k}}^{\text{opt}}(\mathbf{r})$  is given by

$$\psi_{m\mathbf{k}}^{\text{opt}}(\mathbf{r}) = \sum_n U_{mn}^{\text{opt}}(\mathbf{k}) \psi_{n\mathbf{k}}(\mathbf{r}), \quad (2)$$

where  $U_{mn}^{\text{opt}}(\mathbf{k})$  is the projection matrix. The Bloch wave function  $\psi_{n\mathbf{k}}(\mathbf{r})$  is defined as

$$\psi_{n\mathbf{k}}(\mathbf{r}) = \frac{1}{\sqrt{N_{\mathbf{k}}}} \frac{1}{\sqrt{\Omega}} \sum_{\mathbf{G}} C_{Gn}(\mathbf{k}) e^{i(\mathbf{k} + \mathbf{G}) \cdot \mathbf{r}}, \quad (3)$$

where  $\Omega$  is the volume of the calculation unit cell and  $C_{Gn}(\mathbf{k})$  is the expansion coefficient of the plane wave.

Here, we explain the difference between the **Wannier90** and **RESPACK** formats of Wannier functions. By substituting the definition of the Bloch functions into Eq. (1) for  $\mathbf{R} = \mathbf{0}$ , we obtain

$$w_{i0}(\mathbf{r}) = \frac{1}{N_{\mathbf{k}}} \sum_{\mathbf{k}} \sum_{\mathbf{G}} \tilde{C}_{Gi}(\mathbf{k}) \frac{1}{\sqrt{\Omega}} e^{i(\mathbf{k} + \mathbf{G}) \cdot \mathbf{r}}. \quad (4)$$

The relation between  $\tilde{C}_{Gi}(\mathbf{k})$  and  $C_{Gn}$  is

$$\tilde{C}_{Gi}(\mathbf{k}) = \sum_{m,n} U_{im}(\mathbf{k}) U_{mn}^{\text{opt}}(\mathbf{k}) C_{Gn}(\mathbf{k}). \quad (5)$$

The Wannier functions in **RESPACK** are defined in Eq. (4) and used in the calculations of the screened Coulomb interactions. **RESPACK** reads wave functions in the irreducible Brillouin zone (IBZ),  $C_{Gn}(\mathbf{k})$ , where  $\mathbf{k} \in \text{IBZ}$ , to reduce the computational cost, particularly that of the dielectric function. Since crystal symmetry is not taken into account in the standard Wannierization procedure[75],  $U_{im}(\mathbf{k})$ ,  $U_{mn}^{\text{opt}}(\mathbf{k})$ , and  $\tilde{C}_{Gi}(\mathbf{k})$  are calculated on the full  $\mathbf{k}$ -point mesh by expanding  $C_{Gn}(\mathbf{k})$  in the IBZ to the full  $\mathbf{k}$ -point mesh. When using **wan2respack**, we first calculate wave functions in the IBZ,  $C_{Gn}(\mathbf{k})$ , to compute the dielectric function. Then, we separately calculate wave functions on the full  $\mathbf{k}$ -point mesh and generate Wannier functions using Quantum ESPRESSO and Wannier90. **wan2respack** computes  $\tilde{C}_{Gi}(\mathbf{k})$  based on these outputs. Here, we have to use the same full  $\mathbf{k}$ -point mesh used in **RESPACK**.

After the Wannier functions are obtained, the following *ab initio* Hamiltonians are derived:

$$\begin{aligned} H = & \sum_{\sigma, \mathbf{R}\mathbf{R}', \alpha\beta} t_{\alpha\mathbf{R}, \beta\mathbf{R}'} c_{\alpha\mathbf{R}\sigma}^\dagger c_{\beta\mathbf{R}'\sigma} \\ & + \frac{1}{2} \sum_{\sigma\rho, \mathbf{R}\mathbf{R}', \alpha\beta} \left[ U_{\alpha\mathbf{R}, \beta\mathbf{R}'} c_{\alpha\mathbf{R}\sigma}^\dagger c_{\beta\mathbf{R}'\rho}^\dagger c_{\beta\mathbf{R}'\rho} c_{\alpha\mathbf{R}\sigma} \right. \\ & + J_{\alpha\mathbf{R}, \beta\mathbf{R}'} (c_{\alpha\mathbf{R}\sigma}^\dagger c_{\beta\mathbf{R}'\rho}^\dagger c_{\beta\mathbf{R}'\rho} c_{\alpha\mathbf{R}\sigma} \\ & \left. + c_{\alpha\mathbf{R}\sigma}^\dagger c_{\alpha\mathbf{R}\rho}^\dagger c_{\beta\mathbf{R}'\rho} c_{\beta\mathbf{R}'\sigma}) \right], \quad (6) \end{aligned}$$

where  $c_{\alpha\mathbf{R}\sigma}^\dagger$  ( $c_{\alpha\mathbf{R}\sigma}$ ) is a creation (annihilation) operator of the  $\alpha$ th Wannier orbital on  $\mathbf{R}$  with the spin  $\sigma$ . The transfer integral and the screened Coulomb and exchange interactions are defined as

$$t_{\alpha\mathbf{R}, \beta\mathbf{R}'} = \int_V d\mathbf{r} w_{\alpha\mathbf{R}}^*(\mathbf{r}) H_0(\mathbf{r}) w_{\beta\mathbf{R}'}(\mathbf{r}), \quad (7)$$

$$\begin{aligned} U_{\alpha\mathbf{R}, \beta\mathbf{R}'} = & \int_V d\mathbf{r} d\mathbf{r}' w_{\alpha\mathbf{R}}^*(\mathbf{r}) w_{\alpha\mathbf{R}}(\mathbf{r}) \\ & \times W(\mathbf{r}, \mathbf{r}') w_{\beta\mathbf{R}'}^*(\mathbf{r}') w_{\beta\mathbf{R}'}(\mathbf{r}'), \quad (8) \end{aligned}$$

$$\begin{aligned} J_{\alpha\mathbf{R}, \beta\mathbf{R}'} = & \int_V d\mathbf{r} d\mathbf{r}' w_{\alpha\mathbf{R}}^*(\mathbf{r}) w_{\beta\mathbf{R}'}(\mathbf{r}) \\ & \times W(\mathbf{r}, \mathbf{r}') w_{\beta\mathbf{R}'}^*(\mathbf{r}') w_{\alpha\mathbf{R}}(\mathbf{r}'). \quad (9) \end{aligned}$$

Here,  $H_0(\mathbf{r})$  and  $W(\mathbf{r}, \mathbf{r}')$  represent the one-body part of the Hamiltonian (Kohn–Sham Hamiltonian)

and the static screened Coulomb interaction obtained through cRPA, respectively. The integrals are obtained over the crystal volume  $V$ . **RESPACK** calculates these quantities based on the MLWFs.

### 3. Installation of wan2respack

**wan2respack** can be downloaded from the following GitHub repository:

<https://github.com/respack-dev/wan2respack>

Users can compile **wan2respack** using CMake. The typical installation procedure of **wan2respack** is as follows:

```
$ cd $PATH_to_wan2respack
$ mkdir build
$ cd build
$ cmake ../ -DCONFIG=$Type_of_Configure
-DCMAKE_INSTALL_PREFIX=$PATH_to_Install
$ make
$ make install
```

$\$PATH\_to\_wan2respack$  is the path to the **wan2respack** directory and  $\$PATH\_to\_Install$  is the path to the installation directory. By replacing  $\$Type\_of\_Configure$  with the name of CMake configuration files, users can specify their desired compilers.

All binary files and Python scripts are installed to  $\$PATH\_to\_Install/bin$ . The roles of the scripts in **bin** are as follows:

- **init.py**: Common functions are defined in this Python module.
- **qe2respack.py**: This Python script is used to generate the input files of **RESPACK** from the output files obtained by Quantum ESPRESSO band calculations.<sup>1</sup>
- **wan2respack.py**: This is the main Python script. The configuration file name should be written in the **toml** format [76]. This script calls **wan2respack\_pre.py** for preprocessing and **wan2respack\_core.py** for core processing. These scripts are described as follows:

<sup>1</sup>This script is originally distributed under GNU GPL version 3 by the open-source software **RESPACK** version 20200113.

- **wan2respack\_pre.py**: This Python script is used to save the Quantum ESPRESSO results and export  $k$  points with **gen\_mk.x** and **qe2respack.py**.
  - \* **gen\_mk.x**: This execution file, written in Fortran90, for calculating the  $k$ -point mesh for Wannier90.
- **wan2respack\_core.py**: This Python script is used to prepare files about Wannier functions in the RESPACK format using **gen\_wan.x** and **qe2respack.py**.
  - \* **gen\_wan.x**: This execution file, written in Fortran90, converts the Wannier function information in the Wannier90 format into that in the RESPACK format.

#### 4. Usage of wan2respack

The calculation flow of **wan2respack** is as follows:

1. *Ab initio* DFT calculations are performed using Quantum ESPRESSO.
2.  $k$  points are generated for Wannier90 using **wan2respack**.
3. Wannier functions are constructed using Wannier90.
4. The Wannier functions are converted using **wan2respack**.
5. The screened interactions are calculated using RESPACK.

Through these procedures, we obtain the screened Coulomb and exchange interactions in the low-energy effective Hamiltonians of solids. This flow is summarized in Fig. 1.

In the following, we explain the usage of **wan2respack**. The input files for performing these calculations are in **samples/seedname.lattice.kmesh**, where **seedname** is the name of the target compound, **lattice** is the abbreviation of the Bravais lattice, and **kmesh** is the number of  $k$  points. This directory consists of the following directories:

1. **PP**: This includes the pseudopotentials.
2. **inputs**: This includes the input files for self-consistent field (scf) calculations (**seedname.scf.in**), non self-consistent field (nscf) calculations (**seedname.nscf.in**),

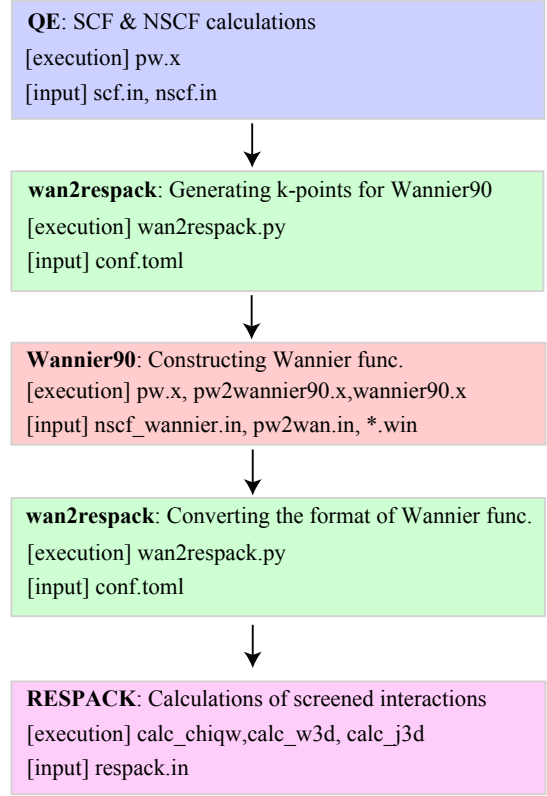


Figure 1: Schematic calculation flow. The necessary executions and input files in each step are also shown.

Wannierization (**seedname.pw2wan.in** and **seedname.win.ref**), and the downfolding by RESPACK (**respack.in**). An input file for **wan2respack** is also included (**conf.toml**). The basic calculation flow is written in **submit.sh**.

3. **inputs\_selfk**: This includes the input files used by the user when setting  $k$  points for Wannier90. The input files for Wannier90 (**seedname.nscf\_wannier.in** and **seedname.win**) are prepared.
4. **reference**: This includes the reference input files for generating the Wannier functions using **calc\_wannier** in RESPACK (RESPACK-Wannier).

##### 4.1. DFT calculations for irreducible $k$ points

DFT calculations of scf and nscf are performed using Quantum ESPRESSO by executing the following commands:

```
$QE/bin/pw.x < seedname.scf.in
               > seedname.scf.out
$QE/bin/pw.x < seedname.nscf.in
               > seedname.nscf.out
```

Here, \$QE indicates a path to the installation directory of Quantum ESPRESSO. The calculated wave functions are used to compute the dielectric function using RESPACK, so  $k$  points should be irreducible to reduce the computational cost.

#### 4.2. Export of $k$ points to be calculated by Wannier90

Next, for preprocessing, we generate a full  $k$ -point list used by RESPACK-Wannier. This  $k$ -point list is exported to the input files of the nscf calculation and Wannier90 by executing the following commands:

```
$python $PATH_to_Install/bin/wan2respack.py
      -pp conf.toml
```

The contents of `conf.toml` are as follows:

```
[base]
QE_output_dir = "./work/seedname.save"
seedname = "seedname"
[pre.ref]
nscf = "seedname.nscf.in"
win = "seedname.win.ref"
[pre.output]
nscf = "seedname.nscf_wannier.in"
win = "seedname.win"
```

`conf.toml` should be written in the toml format [76]. In the [base] section, the output directory of Quantum ESPRESSO and the seed name are specified using `QE_output_dir` and `seedname`, respectively. In the [pre.ref] section, the reference files for generating the input files are specified using `nscf` and `win`, respectively. In the [pre.output] section, the names of the output files generated by `wan2respack` are indicated by `nscf` and `win`. After each calculation, the `dir-wfn` directory and `seedname.nscf_wannier.in` and `seedname.win` files are generated ( $k$  points are added to `seedname.nscf_wannier.in` and `seedname.win`).

#### 4.3. Generation of Wannier functions

Wannier functions are generated using Quantum ESPRESSO, Wannier90, `seedname.nscf_wannier.in`, and `seedname.win` by executing the following commands:

```
$QE/bin/pw.x < seedname.nscf_wannier.in
               > seedname.nscf_wannier.out
$Wannier90/wannier90.x -pp seedname
$QE/bin/pw2wannier90.x < seedname.pw2wan.in
                       > seedname.pw2wan.out
$Wannier90/wannier90.x seedname
```

Here, \$Wannier90 indicates a path to the installation directory of Wannier90.

#### 4.4. Conversion of Wannier functions into RESPACK format

The Wannier functions obtained by Wannier90 are converted into the RESPACK format by executing the following command:

```
$python $PATH_to_Install/bin/wan2respack.py
      conf.toml
```

After these calculations, the following files are generated in the `dir-wan` directory:

- `dat.wan`:  $\tilde{C}_{Gi}(\mathbf{k})$
- `dat.ns-nb`:  $N_s, N_b$
- `dat.umat`:  $\sum_m U(\mathbf{k})_{im} U^{\text{opt}}(\mathbf{k})_{mn}$
- `dat.wan-center`:  $\langle w_{i0} | \mathbf{r} | w_{i0} \rangle$

#### 4.5. Calculation of screened interactions using RESPACK

The input file for RESPACK is `respack.in`. Using this file, we can calculate the screened Coulomb and exchange interactions through cRPA in RESPACK. The execution command is as follows:

```
$RESPACK/bin/calc_chiqr < respack.in > LOG.chiqr
$RESPACK/bin/calc_w3d < respack.in > LOG.W3d
$RESPACK/bin/calc_j3d < respack.in > LOG.J3d
```

For comparison, we provide an input file for RESPACK-Wannier in `reference/respack.in`. As shown later, the obtained Wannier functions and screened interactions by Wannier90 and RESPACK quantitatively agree.

## 5. Application Examples

In this section, we show the application of `wan2respack` to typical compounds for correlated electron systems, namely,  $\text{SrVO}_3$  and  $\text{La}_2\text{CuO}_4$ , whose crystal structures are shown in Fig. 2. The inputs are uploaded to the GitHub repository as



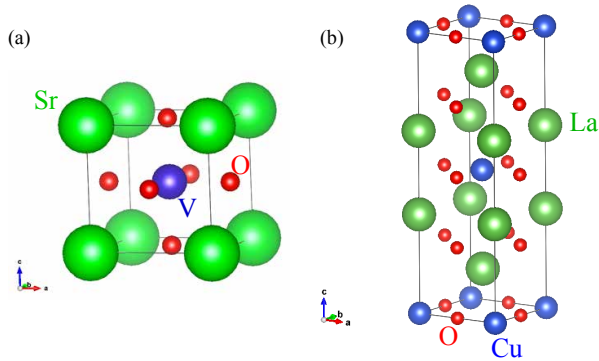


Figure 2: Crystal structures of (a)  $\text{SrVO}_3$  and (b)  $\text{La}_2\text{CuO}_4$  visualized by using VESTA[77]. The space groups of  $\text{SrVO}_3$  and  $\text{La}_2\text{CuO}_4$  shown here are  $\text{Pm}\bar{3}\text{m}$  and  $\text{I4}/\text{mmm}$ , respectively.

samples. Some outputs in this section are also available elsewhere[78]. Note that we use only the disentanglement scheme when we construct the Wannier functions by Wannier90. Nevertheless, as we show later, the Wannier functions constructed from Wannier90 and RESPACK show good agreement with each other.

### 5.1. $\text{SrVO}_3$

$\text{SrVO}_3$  is a typical correlated metal compound[79, 80]. Three  $t_{2g}$ -like orbitals are located around the Fermi energy and isolated from the other bands[81]. As seen in Fig. 3(a), the Wannier bands of the  $t_{2g}$  orbitals obtained using RESPACK and Wannier90 reproduce the original DFT band structure well. Figure 3(b) and (c) show Wannier functions with an orbital index  $\alpha = 1$ . The sum of the spreads of all the Wannier orbitals are 5.5161 [ $\text{\AA}^2$ ] for Wannier90 and 5.5156 [ $\text{\AA}^2$ ] for RESPACK<sup>2</sup>. These results suggest that both software can generate the same Wannier orbitals quantitatively.

Since RESPACK and Wannier90 obtain almost the same Wannier functions, the effective interactions obtained using either Wannier function should be the same if wan2respack works correctly. To confirm this statement, we plot an effective Coulomb interaction written in `dat.WvsR.001` in Fig. 4. The two results show excellent agreement, which indicates that wan2respack works well.

<sup>2</sup>As the unit of the spread, the square of the Bohr radius  $a_0^2$  is employed in the outputs of RESPACK.

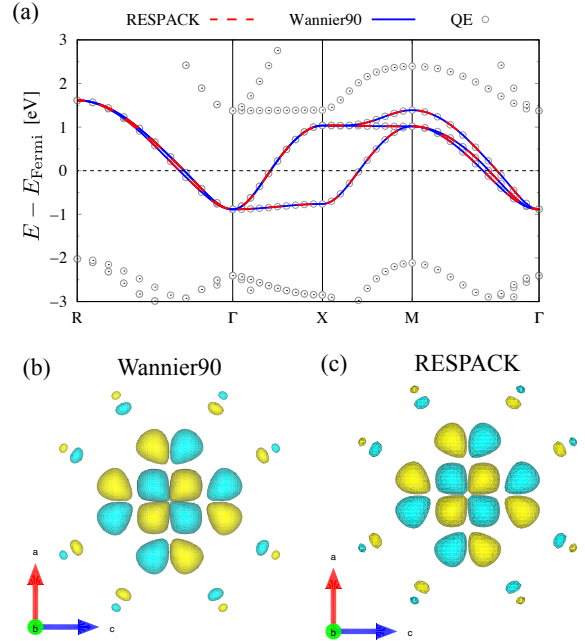


Figure 3: (a) Band structure of  $\text{SrVO}_3$  interpolated by Wannier functions. The blue and red lines show the results obtained using Wannier90 and RESPACK, respectively.  $E_{\text{Fermi}}$  denotes the Fermi energy. The dashed black line represents the Fermi level. The coordinates of the high-symmetry  $\mathbf{k}$ -points in the horizontal axis are  $\Gamma = (0, 0, 0)$ ,  $\text{R} = (0.5, 0.5, 0.5)$ ,  $\text{X} = (0.5, 0, 0)$  and  $\text{M} = (0.5, 0.5, 0)$ . The gray circles depict the band structure obtained using Quantum ESPRESSO. Wannier functions with  $\alpha = 1$  of  $\text{SrVO}_3$  obtained by (b) Wannier90 and (c) RESPACK. The square root of the volume  $1/\sqrt{\Omega}$  is included in the definition of Wannier functions in RESPACK but not in the definition of Wannier functions in Wannier90. See also Eq. (4). This figure is visualized using VESTA[77].

### 5.2. $\text{La}_2\text{CuO}_4$

We show the application of wan2respack to  $\text{La}_2\text{CuO}_4$ , which is a parent compound of high- $T_c$  cuprate superconductors[82, 83]. Although this compound is a Mott insulator of an antiferromagnetic order, most of the DFT results suggest that this compound is a paramagnetic metal in its ground state[84, 85]. In contrast to the DFT calculations, it is shown that the Mott insulating state can be reproduced by solving the effective Hamiltonians derived from *ab initio* downfolding [36, 86].

Compared with  $\text{SrVO}_3$ ,  $\text{La}_2\text{CuO}_4$  has a more complicated band structure[36, 84, 85]. The  $d_{x^2-y^2}$  orbital of copper hybridized with the  $p$  orbitals of oxygen crosses the Fermi energy. Contrary to that of  $\text{SrVO}_3$ , this band is not well isolated: the other bands, such as the  $d_{3z^2-r^2}$  orbital of copper and

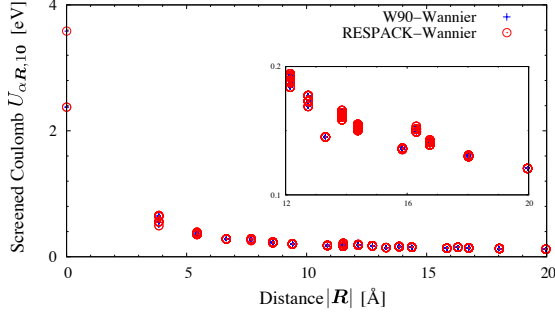


Figure 4: Distance dependence of screened Coulomb interactions  $U_{\alpha\mathbf{R},\beta\mathbf{R}'}$  obtained via cRPA for  $\beta = 1$  and  $\mathbf{R}' = \mathbf{0}$ . W90-Wannier and RESPACK-Wannier indicate the numerical findings from using the Wannier functions obtained by **Wannier90** and **RESPACK**. The inset shows an enlarged view of the Coulomb interactions.

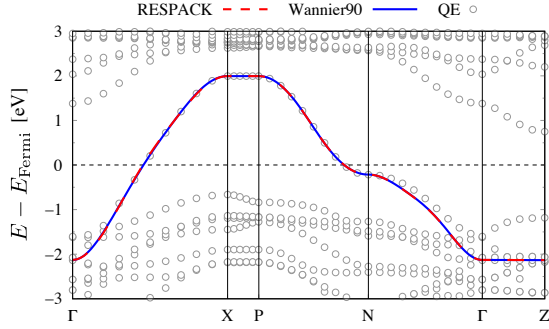


Figure 5: Band structure of  $\text{La}_2\text{CuO}_4$  interpolated using Wannier functions. The coordinates of the high-symmetry  $\mathbf{k}$ -points in the horizontal axis are  $\Gamma = (0, 0, 0)$ ,  $X = (0, 0, 0.5)$ ,  $P = (0.25, 0.25, 0.25)$ ,  $N = (0, 0.5, 0)$ , and  $Z = (0.5, 0.5, -0.5)$ . The notations are the same as in Fig. 3(a).

the  $p$  orbitals of oxygen, exist near the Fermi energy. Such complexity of band structures sometimes leads to difficulties in constructing Wannier orbitals. Nevertheless, as shown in Fig. 5, the band structures near the Fermi level generated by **RESPACK** and **Wannier90** are consistent with each other. We also confirm that the Wannier spreads are also consistent with each other ( $4.0231 \text{ [\AA}^2]$  for **Wannier90** and  $4.0235 \text{ [\AA}^2]$  for **RESPACK**). Moreover, we confirm that the effective interactions calculated via **wan2respac** agree well with the original **RESPACK** results, as shown in Fig. 6.

## 6. Summary

We developed the interface tool **wan2respac**, which converts Wannier functions in the **Wannier90**

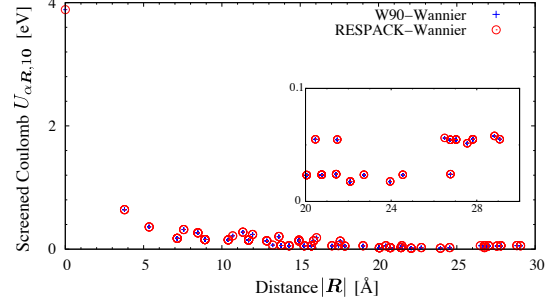


Figure 6: Distance dependence of screened Coulomb interactions  $U_{\alpha\mathbf{R},10}$  for  $\text{La}_2\text{CuO}_4$  obtained via cRPA. We plot only the data for  $|\mathbf{R}| \leq 30$  [87]. The notations are the same as in Fig. 4.

format into those in the **RESPACK** format. Using **wan2respac**, one can perform **RESPACK** calculations using the Wannier functions obtained by **Wannier90**. For example, one can obtain the *ab initio* low-energy effective Hamiltonians of solids using **RESPACK**. To demonstrate the use of **wan2respac**, we derive low-energy effective Hamiltonians for the correlated metal  $\text{SrVO}_3$  and the high- $T_c$  superconductor  $\text{La}_2\text{CuO}_4$  using Wannier functions obtained by **Wannier90** and those obtained by **RESPACK-Wannier**. From these applications, we confirm that the low-energy effective Hamiltonians derived through both implementations of Wannier functions are the same. Since **Wannier90** is a standard tool for constructing Wannier functions, the connection between **Wannier90** and **RESPACK** via **wan2respac** further enhances the usability of **RESPACK**.

## Acknowledgments

We are indebted to Kazuma Nakamura for valuable discussions and for providing us with several codes. We acknowledge Tetsuya Shoji, Noritsugu Sakuma, and Tetsuya Fukushima for fruitful discussions and important suggestions. A part of this work is financially supported by TOYOTA MOTOR CORPORATION. KY and TM were supported by Building of Consortia for the Development of Human Resources in Science and Technology from the MEXT of Japan. We thank Oakbridge-CX in the Information Technology Center, the University of Tokyo and the Supercomputer Center, the Institute for Solid State Physics, the University of Tokyo for their facilities. This

work has also been supported by JST-Mirai Program (JPMJMI20A1), Grant-in-Aid for Scientific Research (Nos. 21H01003, 21H01041, 21H04437, 22K03447, and 22K18954) from Ministry of Education, Culture, Sports, Science and Technology, Japan, and the National Natural Science Foundation of China (Grant No. 12150610462).

## References

- [1] N. Marzari, A. A. Mostofi, J. R. Yates, I. Souza, D. Vanderbilt, [Maximally localized Wannier functions: Theory and applications](#), Rev. Mod. Phys. 84 (2012) 1419–1475.
- [2] N. Marzari, D. Vanderbilt, [Maximally localized generalized Wannier functions for composite energy bands](#), Phys. Rev. B 56 (1997) 12847–12865.
- [3] I. Souza, N. Marzari, D. Vanderbilt, [Maximally localized Wannier functions for entangled energy bands](#), Phys. Rev. B 65 (2001) 035109.
- [4] R. D. King-Smith, D. Vanderbilt, [Theory of polarization of crystalline solids](#), Phys. Rev. B 47 (1993) 1651–1654.
- [5] R. Resta, [Macroscopic polarization in crystalline dielectrics: the geometric phase approach](#), Rev. Mod. Phys. 66 (1994) 899–915.
- [6] T. Thonhauser, D. Ceresoli, D. Vanderbilt, R. Resta, [Orbital magnetization in periodic insulators](#), Phys. Rev. Lett. 95 (2005) 137205.
- [7] D. Xiao, J. Shi, Q. Niu, [Berry phase correction to electron density of states in solids](#), Phys. Rev. Lett. 95 (2005) 137204.
- [8] J. R. Yates, X. Wang, D. Vanderbilt, I. Souza, [Spectral and fermi surface properties from wannier interpolation](#), Phys. Rev. B 75 (2007) 195121.
- [9] F. Aryasetiawan, M. Imada, A. Georges, G. Kotliar, S. Biermann, A. I. Lichtenstein, [Frequency-dependent local interactions and low-energy effective models from electronic structure calculations](#), Phys. Rev. B 70 (2004) 195104.
- [10] M. Imada, T. Miyake, [Electronic structure calculation by first principles for strongly correlated electron systems](#), J. Phys. Soc. Jpn. 79 (11) (2010) 112001.
- [11] P. Hohenberg, W. Kohn, [Inhomogeneous electron gas](#), Phys. Rev. 136 (1964) B864–B871.
- [12] W. Kohn, L. J. Sham, [Self-consistent equations including exchange and correlation effects](#), Phys. Rev. 140 (1965) A1133–A1138.
- [13] K. Nakamura, R. Arita, M. Imada, [Ab initio derivation of low-energy model for iron-based superconductors lafeaso and lafepo](#), J. Phys. Soc. Jpn. 77 (9) (2008) 093711.
- [14] K. Nakamura, T. Koretsune, R. Arita, [Ab initio derivation of the low-energy model for alkali-cluster-loaded sodalites](#), Phys. Rev. B 80 (2009) 174420.
- [15] K. Nakamura, Y. Yoshimoto, T. Kosugi, R. Arita, M. Imada, [Ab initio derivation of low-energy model for  \$\kappa\$ -ET type organic conductors](#), J. Phys. Soc. Jpn. 78 (8) (2009) 083710–083710.
- [16] T. Miyake, K. Nakamura, R. Arita, M. Imada, [Comparison of ab initio low-energy models for LaFePO, LaFeAsO, BaFe<sub>2</sub>As<sub>2</sub>, LiFeAs, FeSe, and FeTe: electron correlation and covalency](#), J. Phys. Soc. Jpn. 79 (4) (2010) 044705.
- [17] T. Misawa, K. Nakamura, M. Imada, [Magnetic Properties of \*Ab initio\* Model of Iron-Based Superconductors LaFeAsO](#), J. Phys. Soc. Jpn. 80 (2) (2011) 023704.
- [18] Y. Nohara, K. Nakamura, R. Arita, [Ab initio derivation of correlated superatom model for potassium loaded zeolite a](#), J. Phys. Soc. Jpn. 80 (12) (2011) 124705.
- [19] T. O. Wehling, E. Şaşıoğlu, C. Friedrich, A. I. Lichtenstein, M. I. Katsnelson, S. Blügel, [Strength of effective coulomb interactions in graphene and graphite](#), Phys. Rev. Lett. 106 (2011) 236805.
- [20] E. Şaşıoğlu, C. Friedrich, S. Blügel, [Strength of the effective coulomb interaction at metal and insulator surfaces](#), Phys. Rev. Lett. 109 (2012) 146401.
- [21] K. Nakamura, Y. Yoshimoto, M. Imada, [Ab initio two-dimensional multiband low-energy models of EtMe<sub>3</sub>Sb\[Pd\(dmit\)<sub>2</sub>\]<sub>2</sub> and  \$\kappa\$ -\(BEDT-TTF\)<sub>2</sub>Cu\(NCS\)<sub>2</sub> with comparisons to single-band models](#), Phys. Rev. B 86 (2012) 205117.
- [22] Y. Nomura, K. Nakamura, R. Arita, [Ab initio derivation of electronic low-energy models for c<sub>60</sub> and aromatic compounds](#), Phys. Rev. B 85 (2012) 155452.
- [23] L. Vaugier, H. Jiang, S. Biermann, [Hubbard \*u\* and hund exchange \*j\* in transition metal oxides: Screening versus localization trends from constrained random phase approximation](#), Phys. Rev. B 86 (2012) 165105.
- [24] R. Arita, J. Kuneš, A. V. Kozhevnikov, A. G. Eguiluz, M. Imada, [Ab initio Studies on the Interplay between Spin-Orbit Interaction and Coulomb Correlation in Sr<sub>2</sub>IrO<sub>4</sub> and Ba<sub>2</sub>IrO<sub>4</sub>](#), Phys. Rev. Lett. 108 (2012) 086403.
- [25] H. Shinaoka, T. Misawa, K. Nakamura, M. Imada, [Mott Transition and Phase Diagram of  \$\kappa\$ -\(BEDT-TTF\)<sub>2</sub>Cu\(NCS\)<sub>2</sub> Studied by Two-Dimensional Model Derived from \*Ab initio\* Method](#), J. Phys. Soc. Jpn. 81 (3) (2012) 034701.
- [26] F. Nilsson, R. Sakuma, F. Aryasetiawan, [Ab initio calculations of the Hubbard \*U\* for the early lanthanides using the constrained random-phase approximation](#), Phys. Rev. B 88 (2013) 125123.
- [27] P. Hansmann, L. Vaugier, H. Jiang, S. Biermann, [What about \*U\* on surfaces? Extended Hubbard models for adatom systems from first principles](#), J. Phys. Condens. Matter 25 (9) (2013) 094005.
- [28] Y. Yamaji, Y. Nomura, M. Kurita, R. Arita, M. Imada, [First-principles study of the honeycomb-lattice iridates na<sub>2</sub>iro<sub>3</sub> in the presence of strong spin-orbit interaction and electron correlations](#), Phys. Rev. Lett. 113 (2014) 107201.
- [29] S. Okamoto, W. Zhu, Y. Nomura, R. Arita, D. Xiao, N. Nagaosa, [Correlation effects in \(111\) bilayers of perovskite transition-metal oxides](#), Phys. Rev. B 89 (2014) 195121.
- [30] B. Amadon, T. Applencourt, F. Bruneval, [Screened coulomb interaction calculations: crpa implementation and applications to dynamical screening and self-consistency in uranium dioxide and cerium](#), Phys. Rev. B 89 (2014) 125110.
- [31] M. Kim, Y. Nomura, M. Ferrero, P. Seth, O. Parcollet, A. Georges, [Enhancing superconductivity in A<sub>3</sub>C<sub>60</sub> fullerides](#), Phys. Rev. B 94 (2016) 155152.
- [32] P. Seth, P. Hansmann, A. van Roekeghem, L. Vaugier, S. Biermann, [Towards a first-principles determination of effective coulomb interactions in correlated electron materials: Role of intershell interactions](#), Phys. Rev. Lett. 119 (2017) 056401.



- [33] M. Hirayama, Y. Yamaji, T. Misawa, M. Imada, *Ab initio effective hamiltonians for cuprate superconductors*, Phys. Rev. B 98 (2018) 134501.
- [34] J.-B. Morée, B. Amadon, *First-principles calculation of coulomb interaction parameters for lanthanides: Role of self-consistence and screening processes*, Phys. Rev. B 98 (2018) 205101.
- [35] T. Tadano, Y. Nomura, M. Imada, *Ab initio derivation of an effective Hamiltonian for the  $\text{La}_2\text{CuO}_4/\text{La}_{1.55}\text{Sr}_{0.45}\text{CuO}_4$  heterostructure*, Phys. Rev. B 99 (2019) 155148.
- [36] M. Hirayama, T. Misawa, T. Ohgoe, Y. Yamaji, M. Imada, *Effective hamiltonian for cuprate superconductors derived from multiscale ab initio scheme with level renormalization*, Phys. Rev. B 99 (2019) 245155.
- [37] Y. Nomura, M. Hirayama, T. Tadano, Y. Yoshimoto, K. Nakamura, R. Arita, *Formation of a two-dimensional single-component correlated electron system and band engineering in the nickelate superconductor  $\text{NdNiO}_2$* , Phys. Rev. B 100 (2019) 205138.
- [38] M. Hirayama, T. Tadano, Y. Nomura, R. Arita, *Materials design of dynamically stable  $d^9$  layered nickelates*, Phys. Rev. B 101 (2020) 075107.
- [39] A. A. Mostofi, J. R. Yates, Y.-S. Lee, I. Souza, D. Vanderbilt, N. Marzari, *wannier90: A tool for obtaining maximally-localised wannier functions*, Comput. Phys. Commun. 178 (9) (2008) 685–699.
- [40] A. A. Mostofi, J. R. Yates, G. Pizzi, Y.-S. Lee, I. Souza, D. Vanderbilt, N. Marzari, *An updated version of wannier90: A tool for obtaining maximally-localised wannier functions*, Comput. Phys. Commun. 185 (8) (2014) 2309–2310.
- [41] G. Pizzi, V. Vitale, R. Arita, S. Blügel, F. Freimuth, G. Géranton, M. Gibertini, D. Gresch, C. Johnson, T. Koretsune, J. Ibañez-Azpiroz, H. Lee, J.-M. Lihm, D. Marchand, A. Marrazzo, Y. Mokrousov, J. I. Mustafa, Y. Nohara, Y. Nomura, L. Paulatto, S. Poncé, T. Ponweiser, J. Qiao, F. Thöle, S. S. Tsirkin, M. Wierzbowska, N. Marzari, D. Vanderbilt, I. Souza, A. A. Mostofi, J. R. Yates, *Wannier90 as a community code: new features and applications*, J. Phys. Condens. Matter 32 (16) (2020) 165902.
- [42] <http://www.wannier.org>.
- [43] X. Wang, J. R. Yates, I. Souza, D. Vanderbilt, *Ab initio calculation of the anomalous hall conductivity by wannier interpolation*, Phys. Rev. B 74 (2006) 195118.
- [44] G. Pizzi, D. Volja, B. Kozinsky, M. Fornari, N. Marzari, *Boltzmann: A code for the evaluation of thermoelectric and electronic transport properties with a maximally-localized wannier functions basis*, Comput. Phys. Commun. 185 (1) (2014) 422–429.
- [45] J. Qiao, J. Zhou, Z. Yuan, W. Zhao, *Calculation of intrinsic spin hall conductivity by wannier interpolation*, Phys. Rev. B 98 (2018) 214402.
- [46] P. Giannozzi, O. Andreussi, T. Brumme, O. Bunau, M. B. Nardelli, M. Calandra, R. Car, C. Cavazzoni, D. Ceresoli, M. Cococcioni, et al., *Advanced capabilities for materials modelling with Quantum ESPRESSO*, J. of Phys.: Cond. Matt. 29 (46) (2017) 465901.
- [47] <https://www.quantum-espresso.org>.
- [48] G. Kresse, J. Furthmüller, *Efficiency of ab-initio total energy calculations for metals and semiconductors using a plane-wave basis set*, Comput. Mater. Sci. 6 (1) (1996) 15–50.
- [49] G. Kresse, J. Furthmüller, *Efficient iterative schemes for ab initio total-energy calculations using a plane-wave basis set*, Phys. Rev. B 54 (1996) 11169–11186.
- [50] P. Blaha, K. Schwarz, F. Tran, R. Laskowski, G. K. H. Madsen, L. D. Marks, *Wien2k: An apw+lo program for calculating the properties of solids*, J. Chem. Phys. 152 (7) (2020) 074101.
- [51] X. Gonze, B. Amadon, G. Antonius, F. Arnardi, L. Baguet, J.-M. Beuken, J. Bieder, F. Bottin, J. Bouchet, E. Bousquet, N. Brouwer, F. Bruneval, G. Brunin, T. Cavignac, J.-B. Charraud, W. Chen, M. Côté, S. Cottenier, J. Denier, G. Geneste, P. Ghosez, M. Giantomassi, Y. Gillet, O. Gingras, D. R. Hamann, G. Hautier, X. He, N. Helbig, N. Holzwarth, Y. Jia, F. Jollet, W. Lafargue-Dit-Hauret, K. Lejaeghere, M. A. Marques, A. Martin, C. Martins, H. P. Miranda, F. Naccarato, K. Persson, G. Petretto, V. Planes, Y. Pouillon, S. Prokhorenko, F. Ricci, G.-M. Rignanese, A. H. Romero, M. M. Schmitt, M. Torrent, M. J. van Setten, B. Van Troeye, M. J. Verstraete, G. Zerah, J. W. Zwanziger, *The abinitproject: Impact, environment and recent developments*, Comput. Phys. Commun. 248 (2020) 107042.
- [52] <https://www.openmx-square.org>.
- [53] T. Ozaki, *Variationally optimized atomic orbitals for large-scale electronic structures*, Phys. Rev. B 67 (2003) 155108.
- [54] T. Ozaki, H. Kino, *Numerical atomic basis orbitals from h to kr*, Phys. Rev. B 69 (2004) 195113.
- [55] K. Nakamura, Y. Yoshimoto, Y. Nomura, T. Tadano, M. Kawamura, T. Kosugi, K. Yoshimi, T. Misawa, Y. Motoyama, *RESPACK: An ab initio tool for derivation of effective low-energy model of material*, Comp. Phys. Comm. 261 (2021) 107781.
- [56] <https://sites.google.com/view/kazuma7k6r>.
- [57] Z. Huang, D. Liu, A. Mansikkamäki, V. Vieru, N. Iwahara, L. F. Chibotaru, *Ferromagnetic kinetic exchange interaction in magnetic insulators*, Phys. Rev. Research 2 (2020) 033430.
- [58] T. Misawa, K. Yoshimi, T. Tsumuraya, *Electronic correlation and geometrical frustration in molecular solids: A systematic ab initio study of  $\beta'-x[\text{Pd}(\text{dmit})_2]_2$* , Phys. Rev. Research 2 (2020) 032072.
- [59] K. Masuda, T. Tadano, Y. Miura, *Crucial role of interfacial  $s-d$  exchange interaction in the temperature dependence of tunnel magnetoresistance*, Phys. Rev. B 104 (2021) L180403.
- [60] M. Charlebois, J.-B. Morée, K. Nakamura, Y. Nomura, T. Tadano, Y. Yoshimoto, Y. Yamaji, T. Hasegawa, K. Matsuhira, M. Imada, *Ab initio derivation of low-energy Hamiltonians for systems with strong spin-orbit interaction: Application to  $\text{Ca}_5\text{Ir}_3\text{O}_{12}$* , Phys. Rev. B 104 (2021) 075153.
- [61] K. Ido, Y. Motoyama, K. Yoshimi, T. Misawa, *Data Analysis of Ab initio Effective Hamiltonians in Iron-Based Superconductors — Construction of Predictors for Superconducting Critical Temperature*, J. Phys. Soc. Jpn. 92 (6) (2023) 064702.
- [62] K. Yoshimi, T. Tsumuraya, T. Misawa, *Ab initio derivation and exact diagonalization analysis of low-energy effective hamiltonians for  $\beta'-x[\text{Pd}(\text{dmit})_2]_2$* , Phys. Rev. Research 3 (2021) 043224.
- [63] N. Morishita, Y. Oishi, T. Yamaguchi, K. Kusakabe,  *$S=1$  antiferromagnetic electron-spin systems on hydrogenated phenalenyl-tessellation molecules for material-based quantum-computation resources*, Appl. Phys. Ex-

- press 14 (12) (2021) 121005.
- [64] A. Steinhoff, F. Jahnke, M. Florian, [Microscopic theory of exciton-exciton annihilation in two-dimensional semiconductors](#), Phys. Rev. B 104 (2021) 155416.
  - [65] S. Kanno, T. Tada, T. Utsumi, K. Nakamura, H. Hosono, [Electronic Correlation Strength of Inorganic Electrides from First Principles](#), J. Phys. Chem. Lett. 12 (50) (2021) 12020–12025.
  - [66] K. Ido, K. Yoshimi, T. Misawa, M. Imada, [Unconventional dual 1D–2D quantum spin liquid revealed by ab initio studies on organic solids family](#), npj Quantum Mater. 7 (1) (2022) 48.
  - [67] J.-B. Morée, M. Hirayama, M. T. Schmid, Y. Yamaji, M. Imada, [Ab initio low-energy effective Hamiltonians for the high-temperature superconducting cuprates Bi<sub>2</sub>Sr<sub>2</sub>CuO<sub>6</sub>, Bi<sub>2</sub>Sr<sub>2</sub>CaCu<sub>2</sub>O<sub>8</sub>, HgBa<sub>2</sub>CuO<sub>4</sub>, and CaCuO<sub>2</sub>](#), Phys. Rev. B 106 (2022) 235150.
  - [68] M.-T. Huebsch, Y. Nomura, S. Sakai, R. Arita, [Magnetic structures and electronic properties of cubic-pyrochlore ruthenates from first principles](#), J. Phys. Condens. Matter 34 (19) (2022) 194003.
  - [69] C.-K. Li, G. Chen, [Universal excitonic superexchange in spin-orbit-coupled Mott insulators](#), Europhys. Lett. 139 (5) (2022) 56001.
  - [70] D. Ohki, K. Yoshimi, A. Kobayashi, T. Misawa, [Gap opening mechanism for correlated Dirac electrons in organic compounds  \$\alpha\$ -\(BEDT-TTF\)<sub>2</sub>I<sub>3</sub> and  \$\alpha\$ -\(BEDT-TSeF\)<sub>2</sub>I<sub>3</sub>](#), arXiv preprint arXiv:2209.13460 (2022).
  - [71] K. Yoshimi, T. Misawa, T. Tsumuraya, H. Seo, [Comprehensive \*abinitio\* investigation of the phase diagram of quasi-one-dimensional molecular solids](#), arXiv preprint arXiv:2210.13726 (2022).
  - [72] J. Yamauchi, M. Tsukada, S. Watanabe, O. Sugino, [First-principles study on energetics of c-BN\(001\) reconstructed surfaces](#), Phys. Rev. B 54 (1996) 5586–5603.
  - [73] <https://ma.issp.u-tokyo.ac.jp/en/app/741>.
  - [74] <https://github.com/respack-dev/wan2respack>.
  - [75] When we generate symmetry-adapted Wannier functions, we can expand  $\tilde{C}_{G_i}(\mathbf{k})$  on the IBZ to the full  $\mathbf{k}$ -points mesh by symmetry[88, 89].
  - [76] <https://tomli.io/en>.
  - [77] K. Momma, F. Izumi, [Vesta 3 for three-dimensional visualization of crystal, volumetric and morphology data](#), J. Appl. Crystallogr. 44 (6) (2011) 1272–1276.
  - [78] [https://isspns-gitlab.issp.u-tokyo.ac.jp/kido902/wan2respack\\_paper](https://isspns-gitlab.issp.u-tokyo.ac.jp/kido902/wan2respack_paper).
  - [79] M. Onoda, H. Ohta, H. Nagasawa, [Metallic properties of perovskite oxide SrVO<sub>3</sub>](#), Solid State Commun. 79 (4) (1991) 281–285.
  - [80] I. H. Inoue, O. Goto, H. Makino, N. E. Hussey, M. Ishikawa, [Bandwidth control in a perovskite-type 3d<sup>1</sup>-correlated metal Ca<sub>1-x</sub>Sr<sub>x</sub>VO<sub>3</sub>. I. Evolution of the electronic properties and effective mass](#), Phys. Rev. B 58 (1998) 4372–4383.
  - [81] F. Lechermann, A. Georges, A. Poteryaev, S. Biermann, M. Posternak, A. Yamasaki, O. K. Andersen, [Dynamical mean-field theory using Wannier functions: A flexible route to electronic structure calculations of strongly correlated materials](#), Phys. Rev. B 74 (2006) 125120.
  - [82] J. G. Bednorz, K. A. Müller, [Possible high-\*T<sub>c</sub>\* superconductivity in the Ba-La-Cu-O system](#), Z. Phys. B: Condens. Matter 64 (2) (1986) 189–193.
  - [83] B. Keimer, S. A. Kivelson, M. R. Norman, S. Uchida, J. Zaanen, [From quantum matter to high-temperature superconductivity in copper oxides](#), Nature 518 (7538) (2015) 179–186.
  - [84] L. F. Mattheiss, [Electronic band properties and superconductivity in La<sub>2-y</sub>X<sub>y</sub>CuO<sub>4</sub>](#), Phys. Rev. Lett. 58 (1987) 1028–1030.
  - [85] W. E. Pickett, [Electronic structure of the high-temperature oxide superconductors](#), Rev. Mod. Phys. 61 (1989) 433–512.
  - [86] T. Ohgoe, M. Hirayama, T. Misawa, K. Ido, Y. Yamaji, M. Imada, [Ab initio study of superconductivity and inhomogeneity in a Hg-based cuprate superconductor](#), Phys. Rev. B 101 (2020) 045124.
  - [87] The long-range part of the screened Coulomb interactions for  $|\mathbf{R}| > 30$  may be meaningless due to the boundary effect of the supercell.
  - [88] R. Sakuma, [Symmetry-adapted Wannier functions in the maximal localization procedure](#), Phys. Rev. B 87 (23) (2013) 235109.
  - [89] T. Koretsune, [Construction of maximally-localized Wannier functions using crystal symmetry](#), Comput. Phys. Commun. 285 (2023) 108645.